Virology 536 (2019) 125–133

Contents lists available at ScienceDirect

Virology

journal homepage: www.elsevier.com/locate/virology

The *Spodoptera frugiperda* Sf9 cell line is a heterogeneous population of rhabdovirus-infected and virus-negative cells: Isolation and characterization of cell clones containing rhabdovirus X-gene variants and virus-negative cell clones

Hailun Ma, Subhiksha Nandakumar[1], Eunhae H. Bae[2], Pei-Ju Chin, Arifa S. Khan[*]

Division of Viral Products, Office of Vaccines Research and Review, Center for Biologics Evaluation and Research, U.S. Food and Drug Administration, Silver Spring, MD, 20993, USA

ARTICLE INFO

Keywords:
Spodoptera frugiperda
Sf9 cell line
Sf-rhabdovirus X-gene variants
Sf-rhabdovirus-negative cell clone
Sf-rhabdovirus-positive cell clone

ABSTRACT

The Sf9 cell line is broadly used for manufacturing baculovirus-expressed viral vaccines. We previously reported the presence of a novel, rhabdovirus in the Sf9 cell line, which contained a unique X gene (Sf-rhabdovirus; designated as X^+ in this paper). These results were extended by other reports describing an Sf-rhabdovirus variant in Sf9 cells, which lacked 320 nucleotides encompassing the X-gene and adjacent intergenic region (designated as X^- in this paper), and the development of an Sf-rhabdovirus negative cell line. Here, we report that the Sf9 cell line is a mixed-cell population, based upon isolation of cell clones with distinct phenotypes: Sf-rhabdovirus-negative, X^+, and X^-. We also show that Sf-rhabdovirus X^+ and X^- variants replicate independently in Sf-rhabdovirus-negative cells. These results shed light on the detection of different rhabdovirus variants by different laboratories using Sf9-derived cell clones and confirm that both X^+ and X^- viruses are infectious in rhabdovirus-negative Sf9 cells.

1. Introduction

Insect cell lines from *Spodoptera frugiperda* (Sf) and *Trichoplusia ni* (Tni) are common cell substrates for baculovirus-expressed biological products (Hink, 1970; Kotin, 2011; Smith, Aug 15, 2000; Summers, 1987; van Oers et al., 2015; Vaughn et al., 1977; Vlak and Keus, 1990; Wickham et al., 1992). Sf cell lines include Sf9 and various Sf9-derived cell clones developed by manufacturers of biological products, as well as the parent cell line Sf21 (Vaughn et al., 1977). We previously identified a novel Sf-rhabdovirus expressed in the Sf9 cell line, obtained from American Type Culture Collection (ATCC), using degenerate RT-PCR assays and high-throughput sequencing (HTS) of the transcriptome. Additionally, virus production was confirmed in cell-free supernatant using transmission electron microscopy (TEM) and HTS (Ma et al., 2014). Sf-rhabdovirus contained five canonical structural genes (N, P, M, G and L), characteristic of rhabdoviruses (Walker et al., 2018), and a unique accessory gene of unknown function, located between G and L, which was designated as X (GenBank accession number KF947078; designated as Sf-rhabdovirus X^+ in this paper). Furthermore, analysis of the parent Sf21 cell line indicated the presence of a 6-bp insertion in the L gene, which was absent in the Sf-rhabdovirus X^+ genome (nucleotide position 8533; GenBank accession number KF947078).

The initial discovery of the Sf-rhabdovirus has been extended by identification of an Sf-rhabdovirus variant in Sf9 cells that lacks 320 nucleotides, extending from within the X gene into the intergenic region between X and L (Hashimoto et al., 2017; Haynes, 2015; Maghodia and Jarvis, 2017) (designated as Sf-rhabdovirus X^- in this paper). This variant was found with or without the 6-bp insertion in the L gene, which was identified in the rhabdovirus of the Sf21 cell line. It is noteworthy that wild populations of *S. frugiperda* are infected with genetically diverse strains of Sf-rhabdovirus (Schroeder et al., 2019). Additionally, an Sf-rhabdovirus-negative cell clone (designated as Sf-RVN) was obtained by antiviral drug treatment of Sf9 subclones, and shown to be susceptible to rhabdovirus infection (Maghodia, 2017; Maghodia et al., 2016; Maghodia and Jarvis, 2017). In this paper we

[*] Corresponding author.
E-mail address: arifa.khan@fda.hhs.gov (A.S. Khan).
[1] Marie-Josée and Henry R. Kravis Center for Molecular Oncology, Memorial Sloan Kettering Cancer Center, New York, NY, USA.
[2] Ross University, School of Medicine, Miramar, FL.

https://doi.org/10.1016/j.virol.2019.08.001
Received 12 June 2019; Received in revised form 31 July 2019; Accepted 1 August 2019
Available online 02 August 2019

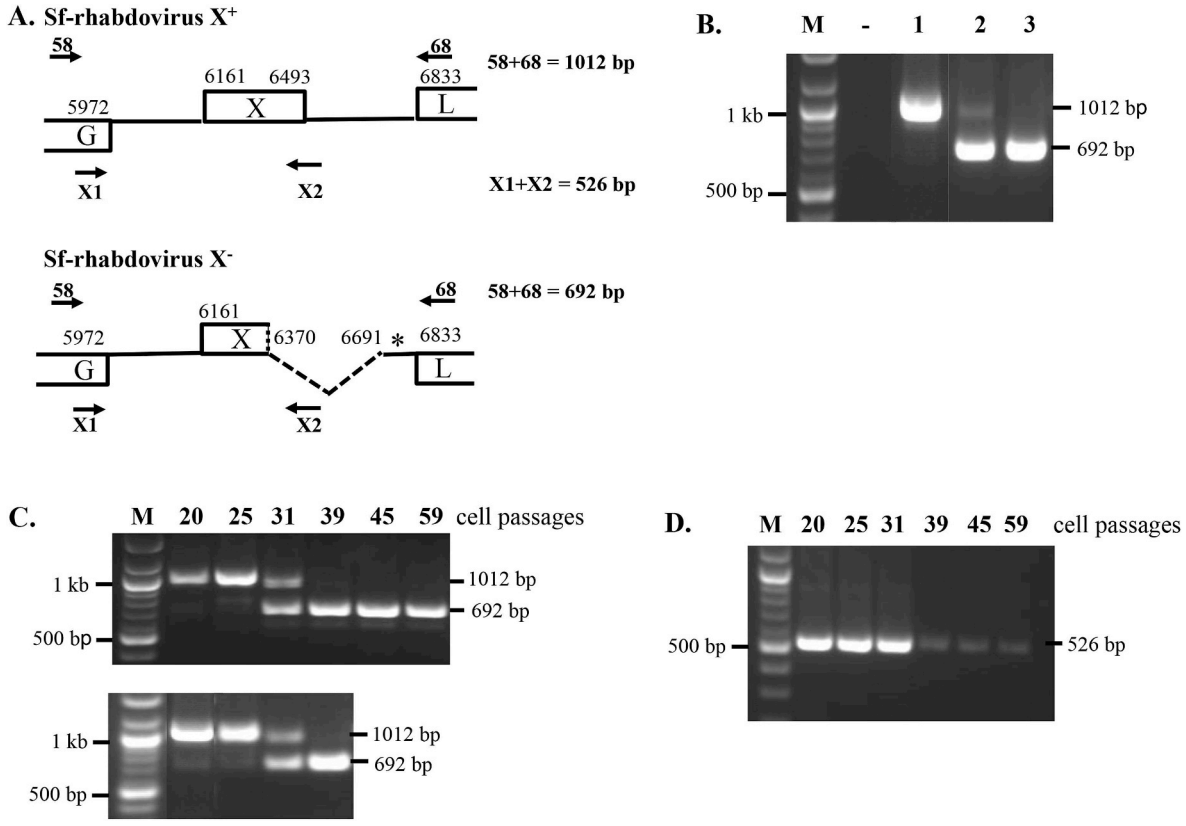

Fig. 1. Analysis of Sf-rhabdovirus X^+ and X^- variants in Sf cell lines. (A) Diagrammatic representation of the X region and adjacent genes in Sf-rhabdovirus X^+ and X^- variants (solid line indicates intergenic regions; broken line indicates absent sequences). PCR primers (arrows) and expected fragment sizes amplified with the different primer pairs are indicated for the X^+ and X^- variants. Nucleotide positions are indicated based upon the published Sf-rhabdovirus genome (Genbank accession number KF947078). The third nucleotide position (6714) of a new stop codon in the X^- variant is indicated by an asterisk. B) Sf-rhabdovirus X^+ and X^- variants were analyzed using total RNAs obtained directly from original, frozen vials of different Sf cell lines: ATCC Sf9 cells (passage 16), Invitrogen Sf9 cells, and Invitrogen Sf21 cells (lanes 1–3, respectively). RT-PCR amplification of total RNAs was done using X gene primers (58 + 68, indicated in panel A and Table 1). Lane -, no template negative control. C) Stability of the Sf-rhabdovirus in the X-gene region was evaluated by RT-PCR analysis of total RNAs obtained from cells (upper panel) or corresponding cell-free supernatant (lower panel) using X-gene primers (58 + 68) at the indicated cell passages. D) RT-PCR amplification of total cell RNAs used in panel C, was done using X-region primers (X1 + X2). 100-bp marker with selected sizes indicated on the left side of the panel (lane M; kb, kilobases, bp, base pair). The size of the PCR-amplified fragments is indicated on the right side of the panels: 1012-bp and 692-bp fragments were amplified using 58 + 68 from X^+ and X^- variants, respectively; a 526-bp fragment was amplified using primers X1 + X2 from the X^+ variant and no product was amplified the X^- variant.

have investigated the occurrence of Sf-rhabdovirus-negative cells and Sf-rhabdovirus X-gene variants using the ATCC Sf9 cell line. The results indicate that Sf9 cells are a mixed population maintaining virus-negative cells alongside cells infected with variant Sf-rhabdoviruses. Furthermore, we describe the isolation of stable, rhabdovirus-negative cell clones and clones producing Sf-rhabdovirus X^+ or X^- viruses. These Sf9 cell clones can aid studies of Sf-rhabdovirus biology and host-cell interactions.

2. Results

X gene analysis in Sf cells. The initial discovery of Sf-rhabdovirus X^+ in the Sf9 cell line from ATCC, which contained an intact X gene, was followed by reports of an Sf-rhabdovirus X^- variant in Sf9 cells that lacked 320 nt between nucleotide positions 6370–6691 (Hashimoto et al., 2017; Haynes, 2015; Maghodia and Jarvis, 2017), including the 5′ part of X gene (120 nt) and 3’ part of intergenic sequences (200 nt), located between the X and L genes. The schematic of the X gene region in the Sf-rhabdovirus, including location of PCR primers used in this study to analyze the Sf-rhabdovirus X^+ and X^- variants and expected fragment sizes, is shown in Fig. 1A. The X gene has a new stop codon at position 6712–6714 nt (accession number KF947078) in Sf-rhabdovirus X^- variant. It should be noted that although the potential transcriptional motif between X and L was deleted in the X^- variant, the L protein open reading frame (ORF) remained intact, but changed from frame 2, which was in the same frame as the intact X gene, to frame 3. This frame-change indicates that the L gene may have used an alternative transcriptional motif located between the G and X genes of Sf-rhabdovirus (position 6114–6128 nt; accession number KF947078).

To specifically investigate whether the X^- variant was present in ATCC Sf9 cells (passage 16), we re-analyzed RNA, which was extracted from the original vial of cryopreserved cells, used in our previous study (Ma et al., 2014). RT-PCR analysis was done using X-gene primers (58 + 68, Fig. 1A and Table 1), which could distinguish Sf-rhabdovirus X^+ and X^- variants. The results indicated amplification of a full-size X gene fragment (1012-bp) (Fig. 1B, lane 1), and confirmed our original HTS data indicating Sf-rhabdovirus X^+ in ATCC Sf9 cells (passage 16). However, PCR analysis of RNA directly extracted from a cryopreserved vial of Sf9 cells obtained from Invitrogen, showed the presence of the X^+ and X^- variants based on amplification of the 1012-bp fragment containing an intact X gene, and the 692-bp fragment, indicative of the X^- virus variant, lacking 320 nt (lane 2). Furthermore, only the X^- variant was detected in the parental Sf21 cell line from Invitrogen (lane 3). The identity of the PCR-amplified fragments was confirmed by direct nucleotide sequencing and analysis. This result is different from previous analysis of the Sf21 cell line, which reported the presence of the Sf-rhabdovirus with an intact X gene, but the source of the cells was not indicated (Maghodia and Jarvis, 2017). However, the latter study

Table 1
PCR primers used for characterization of exogenous and endogenous rhabdovirus sequences.

Primer designation	Sequence[a] (5′ - > 3′)	Nucleotide position[b]	Expected size
Sf-rhabdovirus genome			
Sf-rhabdo-F1	ACTTCACGGATATCGGCTTCT	49-69	
Sf-rhabdo-R1	CAGGGACTCTGTGACCAACC	1223-1204	1175
Sf-rhabdo-F2	AGGAGGAACGGAGAAACCCT	1072-1091	
Sf-rhabdo-R2	TAATGCAGCGGTATAGGCGG	2277-2258	1206
Sf-rhabdo-F3	GCGGAGACACCAGAGGAGAT	2111-2130	
Sf-rhabdo-R3	CCCAAGCTAAGGAAAGGGCA	3289-3270	1179
Sf-rhabdo-F4	AGGAGAACTCCAAAGACTCAGC	3142-3163	
Sf-rhabdo-R4	AAAAGGAGTCCCCACTCAGC	4426-4407	1285
Sf-rhabdo-F5	ACAATCATCCCCTATCGGACT	4249-4269	
Sf-rhabdo-R5	GATCCCTGTGACGGGTTCTG	5513-5494	1265
Sf-rhabdo-F6	AGGTGGTGTTCATCATGGATCT	5357-5378	
Sf-rhabdo-R6	CACTGGCTGTGATGGTAGGT	6332-6313	976
Sf-rhabdo-F7	TCACATCTAGAGCTTGAAGACC	6209-6230	
Sf-rhabdo-R7	TCTGCTCTTGACCACCAGGA	7323-7304	1115
Sf-rhabdo-F8	AGCTAGGGGCATCAGCTACT	7170-7189	
Sf-rhabdo-R8	TCAGGAGGAAACCCTGAGGT	8316-8297	1147
Sf-rhabdo-F9	CCATCTCCTTAGGTTTCCCAGA	8157-8178	
Sf-rhabdo-R9	TCCCAAAGTCCTCGGAGTC	9427-9408	1271
Sf-rhabdo-F10	AGAACCTTCACAGTTGCTTC	9296-9316	
Sf-rhabdo-R10	CAGGACTGATTCCCCCATTGT	10508-10488	1213
Sf-rhabdo-F11	TGCTCAGTTATCAAGGGGGT	10369-10388	
Sf-rhabdo-R11	GTAGGGCTCCCCCAAAAGTC	11529-11510	1161
Sf-rhabdo-F12	TGCACCCTTACAGGGTCATAG	11370-11390	
Sf-rhabdo-R12	CCATCCTTGGATTCCCCGAT	12666-12647	1297
Sf-rhabdo-F13	AGGTCAACTGCAAGAGCTACAA	12514-12535	
Sf-rhabdo-R13	GAGGGTCCACCCTTGATGAC	13454-13435	941
X gene			
Sf-rhabdo-58	GAGAAAGGGGAGGCATCGTT	5877-5896	
Sf-rhabdo-68	TGAGTTGATAAAGGGGGACGTT	6888-6867	1012
Sf-rhabdo-X1	GTTAGGGGGAAACCATGGGG	5949-5965	
Sf-rhabdo-X2	GAGATCACAGGGGTCAGTTTCA	6474-6453	526
Endogenous rhabdovirus[c]			
Sf-EVE-N-F	TGCACAACTAACTGCGGGAT	738-757	
Sf-EVE-N-R	GCCCATACAGCGTCCTCTAC	1298-1279	561
Sf-EVE-P-F	AGGCTCCAAAACCCTGATCG	483-502	
Sf-EVE-P-R	TAGGACCTTCCCAAGAGGGG	984-965	502
Sf-EVE-G-F	ATCGGGTCCAACCCCTTTTC	78-97	
Sf-EVE-G-R	CCCCACCAAACCTCCTAACA	675-656	598
Sf-EVE-L-F	CTAGTCTGTCCTCACTAGCCG	587-607	
Sf-EVE-L-R	TAGATTGACCGCCTCTGGGT	1086-1067	500
Sf 28S ribosomal RNA[d]			
Sf-28S-F	ATAGGGACTGCGAAAGCACG	41-60	
Sf-28S-R	ACTATCGCAACGACAAGCCA	317-298	277

[a] Primer pairs were chosen using Primer BLAST (http://www.ncbi.nlm.nih.gov/tools/primer-blast/).

[b] Nucleotide position is based upon the L protein gene of Sf-rhabdovirus (Genbank accession KF947078).

[c] Primer designed based on *Spodoptera frugiperda* endogenous virus rhabdovirus N-like EVE (Genbank accession KU865648), P-like EVE (KU865649), G-like EVE (KU865646) and L-like EVE (KU865647).

[d] Primer designed based on *Spodoptera frugiperda* 28S ribosomal RNA gene (Genbank accession: EU314585).

corroborated our original results regarding the 6 nt insertion in the L gene in the rhabdovirus in Sf21 cells (Ma et al., 2014).

Since the passage number of the Sf9 and Sf21 cells from Invitrogen was unknown, we investigated the stability of the X^+ and X^- variants upon passage of the ATCC Sf9 cell line (received in our laboratory at passage 16) (Fig. 1C). Analysis of cell RNAs (upper panel), obtained at p20 and p25, by RT-PCR using X-gene primers (58 + 68), indicated amplification of the 1012-bp fragment, indicative of an intact X gene, although a faint 692-bp fragment was also seen indicative of the X^- variant. At p31, fragments corresponding to both X^+ and X^- variants were seen; at p39, the 1012-bp X^+ fragment was barely visible, whereas the 692-bp fragment corresponding to the X^- variant seemed to increase in intensity and persisted at p45 and p59, the last passage tested. Similar results were seen by RT-PCR analysis of the corresponding cell-free supernatants from the passaged cells (Fig. 1C, lower panel). The identity of the 1012-bp PCR-amplified fragment from the cells and supernatant at p20 (Fig. 1C, upper and lower panels, respectively) were confirmed by direct nucleotide sequence analysis. The identity of the faint 692-bp fragment seen in the ATCC Sf9 cells and supernatant at p20 (Fig. 1C, upper and lower panels, respectively) was confirmed by cloning and sequencing; the results indicated the absence of 320 nt in the same location as the variant in the Sf21 cells.

To determine if the lack of detection of the X^+ variant upon further passage of the Sf9 cells may be due to primer competition with the target sequences in the PCR assay, RT-PCR was done using primers X1 + X2, located within the X^- region (Fig. 1A and Table 1), which specifically amplified a 526-bp fragment from the X^+ variant, and no amplification occurred from the X^- variant. The analysis of the same cell RNAs that were used in Fig. 1C (upper panel), showed amplification of the expected 526-bp X-gene fragment (Fig. 1D), indicating the presence of the X^+ variant, which decreased with cell passage, consistent with results seen in Fig. 1C. Interestingly, the internal X^- gene- specific primers detected the X^+ variant in cells at p39, but also at later passages (p45 and p59). The presence of X-gene sequences in the 526-bp fragment was verified by cloning and nucleotide sequence analysis of the PCR-amplified fragment from p59. Similar RT-PCR results were seen with RNAs obtained from ATCC Sf9 cells at passages 27, 31, and 39, after adapting to non-serum conditions according to Invitrogen's protocol (data not shown).

To further evaluate the difference in the X region of Sf-rhabdovirus seen in ATCC Sf9 cells at p20 and at p39 (Fig. 1C), RT-PCR analyses were done using 13 pairs of overlapping primers extending across the Sf-rhabdovirus genome (nucleotides 49–13,454; accession number KF947078) on cell RNAs from p20 and p39 (Fig. 2A and B, respectively). The primer pairs are shown in Table 1 (F1 + R1 through F13 + R13, corresponding to lanes 1 through 13 in Fig. 2A and B). RT-PCR analysis across the virus genome amplified expected-size fragments (indicated in Table 1), except in the region that spanned the X/L region (nt 6209–7323; primers F7 + R7): a 1115-bp fragment indicating presence of the X^+ gene and a faint 795-bp fragment indicating presence of the X^- gene were seen in RNA from p20 cells (Fig. 2A, lane 7), whereas only the X^- gene fragment was seen at p39 (Fig. 2B, lane 7). Sequences in the X^+ and X^- gene fragments were confirmed by nucleotide sequence analysis of the prominent bands in p20 and p39.

Isolation and characterization of Sf9 cell clones. Since Sf9 single-cell clones were not able to survive, limiting dilution method was used for obtaining cell clones that survived with least cell number. Initial cloning was done using ATCC Sf9 cells at passage 30. Out of a total of 115 cell clones obtained from fifteen 96-well plates, 18 were negative for Sf-rhabdovirus at p1 by RT-PCR analysis of cell RNA, while some others contained the Sf-rhabdovirus X^- variant (based on PCR amplification of the 692-bp fragment). Five Sf-rhabdovirus-negative cell clones and 5 cell clones positive for Sf-rhabdovirus X^- variant were selected and cultured further to p10. Three out of the 5 Sf-rhabdovirus-negative cell clones (designated as 13F12, 7F12, and 12H5) remained virus-negative at p10 (Fig. 3A) as well as at p30 (data not shown). Amplification of the expected size 277-bp fragment using 28S rRNA primers (Table 1, Fig. 3A, lower panel) demonstrated presence of cell RNA in the samples. All of the 5 cell clones containing Sf-rhabdovirus X^- variant (designated as 1A3, 1B4, 4A10, 14E8 and 13A3) were positive at p10 (Fig. 3A, upper panel) and at p30 (data not shown). Clone Sf9-13F12 was selected as a representative Sf-rhabdovirus negative cell clone and clone Sf9-1A3 was selected to represent the X^- variant virus.

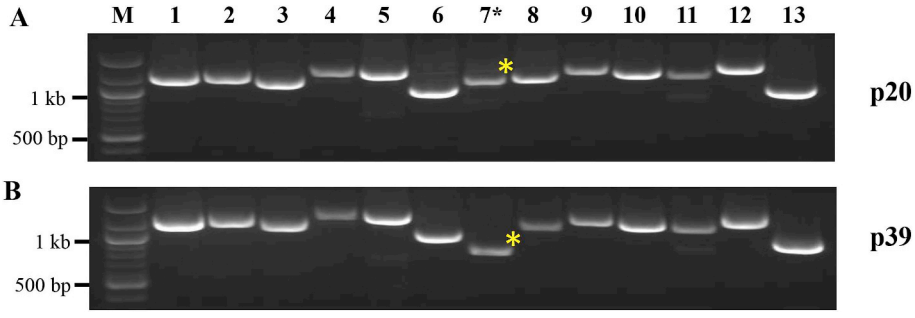

Fig. 2. RT-PCR analysis across Sf-rhabdovirus X^+ and X^- variant genomes. Total cell RNA was extracted from ATCC Sf9 cells at (A) p20 and (B) p39 and RT-PCR analysis done using 13 virus-specific primer pairs that amplified overlapping fragments over the length of the genome (lane numbers correspond to F and R primer numbers in Table 1). Fragments corresponding to an intact X gene (1115 bp) and without 320 nt (795 bp) are shown by an asterisk in panels A and B, respectively (lanes 7, asterisk). Their identities were confirmed by sequencing (data not shown). Lane M, 100-bp marker with selected sizes indicated.

To obtain a cell clone containing Sf-rhabdovirus X^+, a second-round of cloning was done starting from ATCC Sf9 cells at p22, in which the majority of Sf-rhabdovirus was the X^+ variant. From of a total of 19 cell clones, which were obtained from ten 96-well plates, 3 were negative for Sf-rhabdovirus at p1 by RT-PCR analysis of cell RNA, while 11 contained the X^+ variant and 2 had the X^- variant. All of the cell clones were cultured further to p10 and were found to retain the same X^+ or X^- phenotype as in passage p1. The results of the RT-PCR analysis of the RNAs from the Sf9 cell clones at p10 are shown in Fig. 3B (upper panel): three were Sf-rhabdovirus-negative (designated as 2–12, 2–13, 2–19), eleven were X^+, based on amplification of the expected 1012-bp fragment (designated as 2-2, 2–4, 2–5, 2–6, 2–7, 2–8, 2–9, 2–14, 2–15, 2–16, 2–18, 2–20), and two were X^-, based on amplification of the expected 692-bp fragment (designated 2–10, 2–22) at p10. Amplification of the 28S rRNA 277-bp fragment demonstrated presence of cell RNA in the samples (Fig. 3B, lower panel). Clone Sf9-2-20 was selected to represent the X^+ variant.

RT-PCR analysis of cell RNAs obtained from Sf9-13F12 at p9, Sf9-2-20 at p10, and Sf9-1A3 at p10 was done using the 13 overlapping primers across the Sf-rhabdovirus genome (Table 1). The results confirmed the absence of Sf-rhabdovirus sequences in Sf9-13F12 (Fig. 4A) and presence of Sf-rhabdovirus X^+ and X^- variants in clones Sf9-2-20 and Sf9-1A3, respectively (Fig. 4B and C). The variants were identified by amplification of the expected 1115-bp and 795-bp fragments, indicative of X^+ and X^- variants, respectively, using primers F7 + R7, and identity was confirmed by direct sequencing of the PCR amplified fragments. Similar RT-PCR results were seen between virus-negative clones Sf9-13F12 and Sf9-2-19; and X^- cell clones, Sf9-1A3 and Sf9-2-22 (results not shown). To further verify the absence of the X^+ variant in Sf9-1A3, RT-PCR analysis was done using X1 + X2 primers (Table 1). The results confirmed the absence of X^+ in Sf9-1A3 and the expected presence of X^+ in Sf9-2-20 (results not shown). Additionally, direct sequencing of RT-PCR amplified fragments from Sf9-1A3 using primers in the early L region (lane 9) indicated the absence of the 6-bp insertion that was previously found in Sf21 (Ma et al., 2014) and also found in other Sf cell lines (Maghodia and Jarvis, 2017).

Transcriptomic analysis of Sf9-13F12 for rhabdovirus sequences. To confirm the absence of Sf-rhabdovirus in the Sf9-13F12 cell clone, HTS reads obtained from the whole transcriptome were analyzed by blastn search against U-RVDB v12.2 (Goodacre et al., 2018; Khan and Goodacre, 2018). Reads with viral hits were followed-up by initial mapping to the target virus genome as reference including Sf-rhabdovirus. The identity of the hits was verified as viral or non-viral by using the mapped consensus sequences for blastn searches against U-RVDB v12.2, which contains high virus sequence diversity and reduced cellular content (Goodacre et al., 2018), and against NCBI nr/nt, which

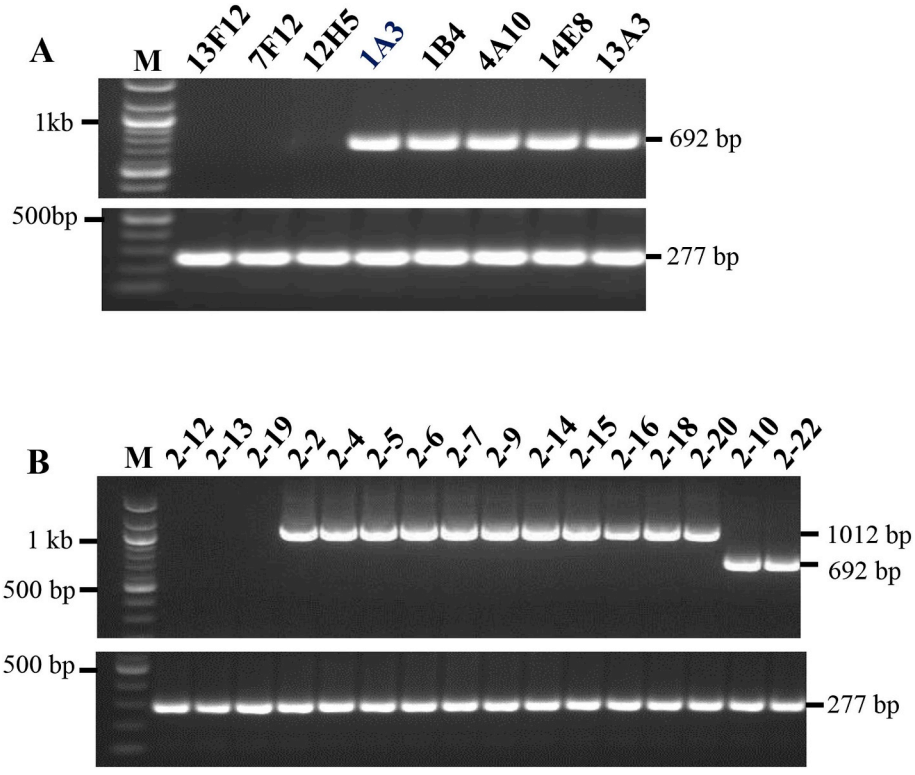

Fig. 3. Isolation and characterization of Sf9 cell clones. (A) Three Sf-rhabdovirus negative (13F12, 7F12, 12H5) and five Sf-rhabdovirus X^- cell clones (1A3, 1B4, 4A10, 14E8, 14A3) were obtained by limiting dilution directly from the ATCC Sf9 cell line at p30. (B) Three Sf-rhabdovirus-negative cell clones (2–12, 2–13, 2–19), eleven Sf-rhabdovirus X^+ cell clones (2-2, 2–4, 2–5, 2–6, 2–7, 2–9, 2–14, 2–15, 2–16, 2–18, 2–20), and two Sf-rhabdovirus X^- cell clones (2–10, 2–22) were obtained by limiting dilution of the ATCC Sf9 cell line at p22. Total RNAs from each clone were analyzed at p10 by RT-PCR assays using X-gene primers (58 + 68) (upper panels in A and B). RT-PCR analysis of RNAs from cell clones using 28S rRNA primers amplified the expected size fragment (277 bp, lower panels in A and B) demonstrated presence of RNAs in the samples. Lanes M, 100-bp marker with selected sizes indicated.

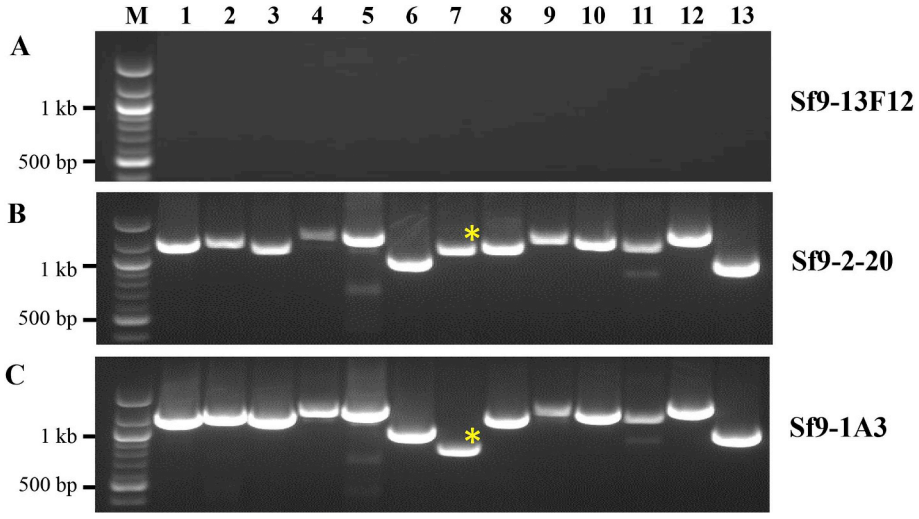

Fig. 4. Characterization of Sf-rhabdovirus genome in Sf9 cell clones. Total cell RNAs were characterized for Sf-rhabdovirus genome by RT-PCR using 13 pairs of overlapping primers for three selected Sf9 cell clones: (A) Sf-rhabdovirus negative clone Sf9-13F12, p9; (B) Sf-rhabdovirus X^+ clone Sf9-2-20, p10; and (C) Sf-rhabdovirus X^- clone Sf9-1A3, p10. Lane M, 100-bp marker with selected sizes indicated. The X^+ gene fragment (1115 bp) and X^- gene fragment (795 bp) are indicated by an asterisk in lane 7 (B and C, respectively).

included all viral and cellular sequences (data not shown). The results confirmed the absence of any rhabdovirus-specific sequences in Sf9-13F12 cells. A re-analysis of the Sf9-13F12 raw reads was done at the time of submitting this paper using the updated RVDB v15.1 (Khan and Chin, 2019). A tblastx search of C-RVDB v15.1 indicated no rhabdovirus-related hits, or hits to the virus family *Mononegavirales*, confirming the absence of an exogenous rhabdovirus in the Sf9-13F12 cells (data not shown). Expectedly, expression of endogenous rhabdovirus-like elements was seen (discussed below).

Characterization of endogenous rhabdovirus-like elements. Endogenous rhabdovirus-like sequences have previously been identified in the Sf9 genome that are related to, but distinct from, the exogenous Sf-rhabdovirus N, P, G, and L genes (Geisler and Jarvis, 2016). The endogenous rhabdovirus sequences expressed in Sf9-13F12 cells were queried against the individual endogenous rhabdovirus genes (accession numbers shown in Table 1) as reference, using blastn and blastx: reads mapped with 100% coverage and 99–100% identify to endogenous rhabdovirus-like N, P, G, and L elements (data not shown). A comparison of the nucleotide sequence and amino acid sequence identity of the exogenous rhabdovirus genes (Sf-rhabdovirus) and endogenous rhabdovirus-like elements (Sf-EVEs) is shown in Tables 2 and 3, respectively. Additionally, the percent of gene sequences covered in the Sf-rhabdovirus is indicated. We further characterized the Sf-EVE genomic loci using our published draft Sf9 assembled genome v1.0 (Nandakumar et al., 2017). Blastn searches using Sf-EVEs as reference sequences indicated N, P, G, and L elements were located on distinct contigs, which ranged in size from about 43,000 bp to over 900,000 bp. It was further noted that the P-like gene was present in 2 contigs and one of the contigs contained 9 copies; L-like genes were present in single copy in two contigs, and G-like and N-like genes were present in single copy in one contig each.

We evaluated the expression of the endogenous rhabdovirus-like elements in the ATCC Sf9 cell line at p20 (same sample used in Fig. 1C) and in the Sf9-13F12 and Sf9-1A3 cell clones by RT-PCR analysis of cDNA from p30. Specific primers were designed based on the published endogenous rhabdovirus-like N, P, G and L elements (Table 1) (Geisler and Jarvis, 2016). RT-PCR analysis showed amplification of the expected size fragments and a similar RNA expression of the Sf-EVE genes was seen in Sf-rhabdovirus-negative Sf9-13F12 cell clone, Sf-rhabdovirus X^- Sf9-1A3 cell clone, and the ATCC parental Sf9 cell line (Fig. 5A). However, no endogenous rhabdovirus-like genes were detected in RNAs prepared from pelleted material from cell-free supernatant of Sf9 p20 (same sample used in Fig. 1C; lower panel) and p30 of the two cell clones (Fig. 5B). These results indicated that expression of endogenous rhabdovirus-like sequences in the Sf-rhabdovirus negative cells was not influenced by infection with Sf-rhabdovirus. Additionally, equivalent DNA PCR amplification of endogenous rhabdovirus-like sequences was seen in the original ATCC Sf9 cell line at p16 and Invitrogen Sf21 cells (Fig. 5C). These results suggested that the endogenous rhabdovirus-like fragments were integrated in the Sf genome and stably expressed during the passages involved in the isolation of the Sf9 subclone from the parent Sf21 cell line.

Infectivity studies of Sf-rhabdovirus X^+ and X^- variants. We used the Sf-rhabdovirus-negative cell clone Sf9-13F12 to investigate the infectivity of rhabdovirus X^+ and X^- variants. Filtered supernatants from Sf9 cells at p20, which predominantly contained the X^+ variant, and at p39, which predominantly contained the X^- variant (Fig. 1C, lower panel), were inoculated into Sf9-13F12 cells. RT-PCR analysis of RNA from inoculated Sf9-13F12 cells showed replication of both Sf-rhabdovirus X^+ and X^- viruses (data not shown). To further investigate whether Sf-rhabdovirus X^+ or X^- can replicate independent of each other, filtered supernatants from Sf9-1A3 cells, which contained only the X^- variant, and from Sf9-2-20 cells, which contained only the X^+ variant (Fig. 3A and B, respectively), were inoculated into Sf9-13F12 cells. RT-PCR results from the inoculated Sf9-13F12 cells showed that Sf-rhabdovirus X^+ and X^- replicated independently and stably in

Table 2
Blastn analysis of exogenous and endogenous rhabdovirus genes.

Gene	Gene length (bp)		Blastn		
	Sf-rhabdovirus	Sf-EVE	Sf-rhabdovirus gene covered (%)	Identity[a]	E-value
N	1566	1512	2	32/38 (84%)	3e-7
P	1146	1137	99	786/1135 (69%)	2e-134
M	927	Not found			
G	1833	1112	58	791/1063 (74%)	0.0
L	6423	1259	20	946/1259 (75%)	0.0

[a] Number of nucleotides in endogenous rhabdovirus gene/number of nucleotides in Sf-rhabdovirus gene; calculated percent identity is indicated in parenthesis.

Table 3
Amino acid analysis of endogenous and exogenous rhabdovirus genes.

Gene	Gene length (aa)		Blastx		
	Sf-rhabdovirus	Sf-EVE	Sf-rhabdovirus gene covered (%)	Identity[a]	E-value
N	521	501	95	175/494 (35%)	4e-94
P	381	378	99	297/378 (79%)	0.0
M	308	Not found			
G	610	363	59	298/362 (82%)	0.0
L	2140	420	20	388/420 (92%)	0.0

[a] Number of amino acids in Sf-rhabdovirus genes/number of amino acids in Sf-EVE gene; calculated percent identity is indicated in parenthesis.

Sf9-13F12 cells for 30 passages, the last tested passage level (Fig. 6, panels A and B, respectively). Interestingly, it was noted that the 1012-bp fragment from X^+ was first seen at p3 whereas the 692-bp fragment from X^- could be detected at p1. Further studies will aid in investigating differences in the replication of the Sf-rhabdovirus variants.

3. Discussion

The discovery of the novel Sf-rhabdovirus in the Sf9 cells containing an intact X gene (designated as Sf-rhabdovirus X^+) (Ma et al., 2014) resulted in further investigations, which identified a variant lacking 320 nt in the X gene and the adjacent intergenic region between X and L (designated as Sf-rhabdovirus X-) (Hashimoto et al., 2017; Haynes, 2015; Maghodia and Jarvis, 2017). Subsequently Sf-rhabdovirus X^+ was found by others (Maghodia and Jarvis, 2017), but the relationship between the X^+ and X^- variants remained unclear. Furthermore, a rhabdovirus-negative cell clone was obtained but details of its origin and derivation were not available (Maghodia et al., 2016), until later (Maghodia, 2017). Therefore, we undertook efforts with the ATCC Sf9 cell line that was used in our initial study for discovery of the Sf-rhabdovirus X^+, to investigate the presence of rhabdovirus variants and potential presence of virus-negative cells. We noticed that the Sf-rhabdovirus X^+ that we discovered in ATCC cells at early passage (p20), decreased upon extended passage of the cells with a concomitant increase of the Sf-rhabdovirus X^- variant (Fig. 1C). Additionally, using X-gene-specific PCR primers, we found that the X^- variant was faintly detected by RT-PCR in the Sf9 cells from ATCC at p20 and the X^+ was faintly detected, even at higher passage (Fig. 1D). Therefore, we initiated studies to determine the percentage of cells infected with the X^+ and X^- virus variants in the ATCC Sf9 cell line and whether cells were co-infected or singly-infected with rhabdovirus, and also investigated whether replication of the variants was co-dependent or independent. These questions were addressed by isolation of cell clones using limiting dilution and initial characterization for Sf-rhabdovirus sequences by RT-PCR analysis. Three distinct cell phenotypes were obtained: Sf-rhabdovirus negative, Sf-rhabdovirus X^+, and Sf-rhabdovirus X^-. Long-term cultures verified that the cell clones were stable and maintained their original virus-negative and virus-variant phenotypes, including a

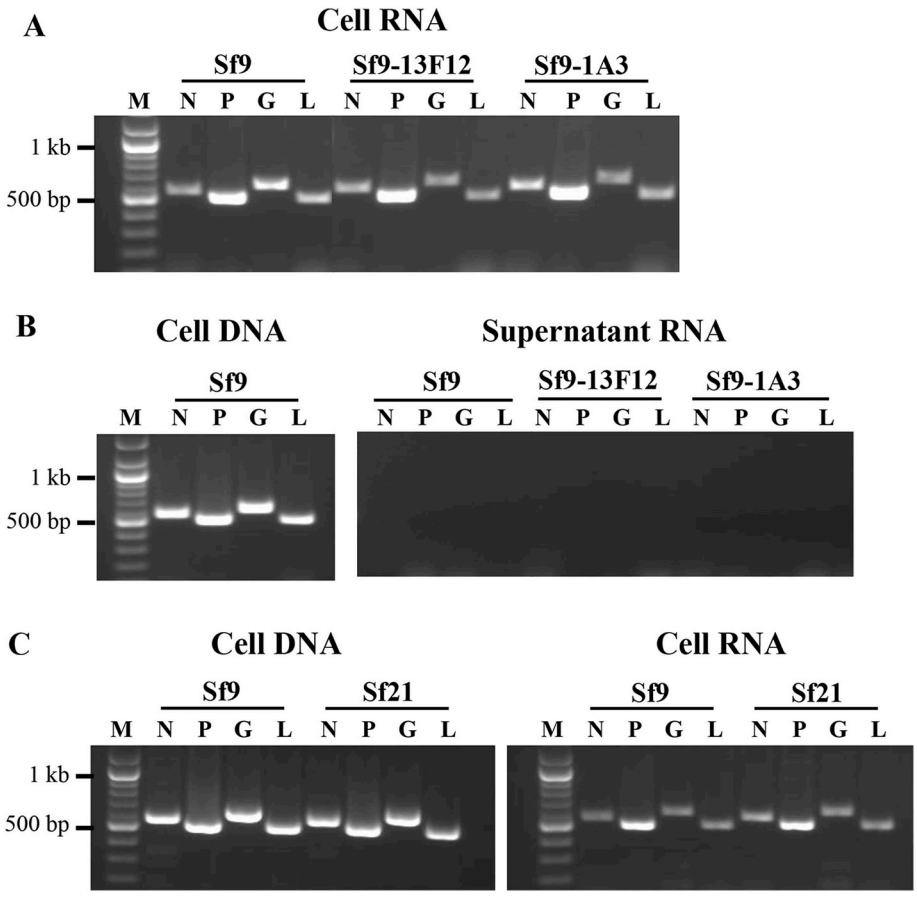

Fig. 5. Characterization of endogenous rhabdovirus-like genes N, P, G, and L in Sf9 cells. RT-PCR was done using primers based on published endogenous rhabdovirus-like genes (Table 1). (A) Total cell RNAs were extracted from Sf9 cells (ATCC, p20), Sf9-13F12 cell clone at p30, and Sf9-1A3 cell clone at p30. (B) Total RNAs extracted from supernatant of corresponding cells shown in panel A. Cell DNA from Sf9 cells at p20 was added as positive control. (C) Cell DNA and RNA were extracted from a cryovial of Sf9 cells from ATCC and Sf21 cells from Invitrogen. Lane M, 100-bp marker with selected sizes indicated.

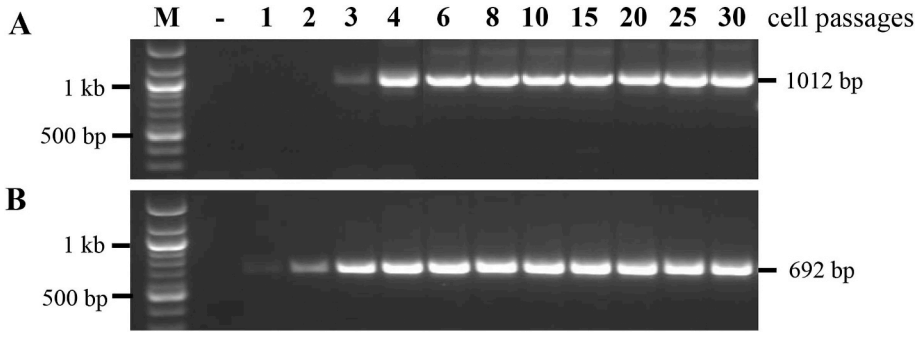

Fig. 6. Replication of Sf-rhabdovirus X^+ or X^- in the Sf9-13F12 cell clone. Sf9-13F12 cells were inoculated with filtered supernatant from clone Sf9-2-20 (X^+, top panel) or from clone Sf9-1A3 (X^-, bottom panel) at p10. RT-PCR analysis of cell RNAs from infected cells at different passages was done using X-gene primers 58 + 68. Lane -: Sf9-13F12 cells without infection. Lane M: 100-bp marker with selected sizes indicated. The size of the PCR-amplified Sf-rhabdovirus fragments (1012 bp for X^+ and 692 bp for X^-) are indicated.

stable X^+ genome. These results demonstrated that the Sf9 cell line is a mixed population of different cell phenotypes consisting of uninfected cells, and cells infected with rhabdovirus X-gene variants. It should be noted that in contrast to a previously isolated rhabdovirus-negative cell clone, which was derived by initial long-term culture and drug-treatment of Sf9 cell clones isolated by limiting dilution (Maghodia, 2017), we were able to directly isolate rhabdovirus-negative cell clones from Sf9 cells by limiting dilution. We also found that single-cell clones did not survive, so our clones are a homogeneous population of cells selected by limiting dilution to obtain a stable phenotype.

The results from the different studies described in this paper indicates that the X^+ variant is "supplanted" by the X^- variant upon extended culture, which could be due to cell growth properties or culture conditions. The dynamics of the Sf9 culture is puzzling since virus-negative cells that are susceptible to virus infection, persist and remain uninfected alongside cells producing infectious virus. This cannot be explained by difference in cell growth since the population doubling time of the virus-negative and virus-positive cells appears to be similar (Maghodia et al., 2016) (unpublished data). Furthermore, the presence or absence of serum in the culture medium (Grace's medium with 10% FBS or using Sf-900™ II SFM serum-free complete medium) did not seem to influence the dynamics of X^+ and X^- variants (data not shown). To investigate if any "resistant" factors were produced from the Sf9-13F12 clone, we used conditioned medium from the Sf9-13F12 clone mixed with virus-containing supernatant from the Sf9 cells and from Sf9 X^+ and X^- clones to infect Sf9-13F12. The results showed successful virus infection with all samples (data not shown). Further investigations are needed to determine different cell-specific properties that may contribute to the maintenance of the cell culture dynamics and persistence of the virus-negative cells in the Sf9 mixed cell population.

All rhabdoviruses have five structural genes N, P, M, G and L and some have additional ORFs, varying in number and locations in the virus genome, and in most cases with unknown function and origin (Walker et al., 2015). We identified the X gene between the canonical G and L genes in Sf-rhabdovirus. Since the lack of 320 nt encompassing the X and X/L intergenic regions do not affect the function of the adjacent L gene and production of infectious virus, it seems that an intact X gene is not critical for Sf-rhabdovirus replication life cycle. Based upon our preliminary results, the population doubling time of the cell clones producing Sf-rhabdovirus X^+ and X^- variants was similar. Therefore, the emergence of the X^- variant with cell passage and decrease in the X^+ variant might be due to better replication of the former virus compared with the latter. If this were the case, then the presence of the additional X gene between G and L could play a role in decreasing L transcription. We have not found any homology of the X sequences to any known sequence by blastn, tblastx and blastp searches in NCBI nucleotide and protein databases.

The results of our study and other published studies regarding characterization of Sf cells and rhabdovirus variants can aid manufacturers using Sf cells for baculovirus-expressed products. The availability of Sf-rhabdovirus sequences can facilitate development of virus-specific PCR assays that can distinguish from endogenous rhabdovirus-sequences, thus giving accurate results about virus contamination of the cells. Testing the starting cells for Sf-rhabdovirus can help design steps in the manufacturing process for testing and removal of the virus to assure purity of the final product (US Food and Drug Adminstration, 2010). Additionally, Sf-rhabdovirus-negative cell clones, that are susceptible to virus infection, provide an important reagent for developing infectivity assays for demonstrating the absence of infectious virus in products produced using Sf cells. We also noted that infection of the cells with the X^+ or X^- variants did not influence expression of the endogenous rhabdovirus-like sequences (Fig. 5A). Although Sf-rhabdovirus has thus far been shown to be infectious only in insect cells and has not been shown to be infectious in mammalian cell lines (Ma et al., 2014; Maghodia and Jarvis, 2017; Schroeder et al., 2019), general recommendations for product purity and safety include clearance of infectious adventitious viruses in biological products (US Food and Drug Adminstration, 2010).

Our initial HTS analysis of the Sf9 p20 transcriptome identified only the Sf-rhabdovirus X^+ (Ma et al., 2014) and the low-level X^- variant was not detected. Re-analysis of the data after reports of the X^- variant from various labs, identified a low number of reads using the X^- region as reference. These results highlight the importance of continued efforts to understand the strengths and limitations of the tools used for HTS bioinformatics and storage of the HTS raw read data for future re-analysis based upon availability of new information. Our results indicated that although HTS can have good sensitivity for virus detection, different bioinformatics tools and strategies may need to be used to identify SNPs versus long indels. We used extensive bioinformatics analysis of the whole transcriptome and RT-PCR assays to demonstrate the absence of Sf-rhabdovirus or a related virus from the family *Mononegavirales* in the Sf9-13F12 cell line. Additional bioinformatics analysis resulted only in the expected detection of endogenous viral sequences or non-viral hits. This study demonstrates that a combination of conventional methods and advanced technologies can provide greater assurance for virus detection and are currently recommended to demonstrate freedom from adventitious viruses for product safety (US Food and Drug Adminstration, 2010).

4. Materials and methods

Cell lines. The Sf9 cell line was obtained from American Type Culture Collection (ATCC, Manassas, VA, catalogue number CRL-1711, lot no. 58078522, passage 16) and grown as an adherent culture in Grace's supplemented insect medium with 10% fetal bovine serum (designated as complete medium in this paper) as previously described (Ma et al., 2014). RNAs, which were previously extracted directly without culturing from frozen Sf9 and Sf21 cells (purchased from ATCC and Invitrogen, respectively), were also used in this study for RT-PCR analysis (Ma et al., 2014).

Cell cloning. Sf-rhabdovirus-negative cell clones and cell clones containing Sf-rhabdovirus X^+ and X^- were obtained by limiting dilution. Two cell clonings were done using ATCC Sf9 cells at p30 and p22.

Sf9 cells were scrapped and resuspended in complete media at a concentration of 10^4 cells per mL. One-hundred microliters were added to the wells in the first column of 96-well plates, which contained 100 µL complete medium in each well and two-fold serial dilutions were made using a multichannel pipette. Cells in each well were observed twice a week and medium changed once a week. Only the cells in each row with the least cell number that reached more than 40% confluence after 6–8 weeks were transferred to 24-well plates. A portion of the cells (two-third) from each confluent well was harvested for RT-PCR analysis to evaluate for presence of Sf-rhabdovirus using X^+ primers (Table 1) and the remainder of cells were further cultured in new 24-well plates. Several selected Sf-rhabdovirus-negative cell clones, Sf-rhabdovirus X^+ and X^- cell clones were cultured by transferring sequentially in 6-well plates, 25-cm^2 flasks, and 75-cm^2 flasks. A portion of the cells from the 75-cm^2 flask was cryopreserved in liquid N2 at p5. The rest of the cells were further cultured in 25-cm^2 until passage 30. The cell clones were tested using RT-PCR assays for Sf-rhabdovirus sequences using X^+ primers at p10 and p30.

After confirming the absence of Sf-rhabdovirus at p10 by RT-PCR analysis, 3 Sf-rhabdovirus-negative clones (designated as 13F12, 7F12 and 12H5) were evaluated further for growth kinetics and susceptibility to rhabdovirus infection. Cryopreserved cells of Sf9-13F12/p5 were further expanded, using the same medium and conditions as for Sf9 cells, by initially growing in a 25-cm^2 flask and upon reaching confluence, transferring to a 75-cm^2 flask and further passaging until p9. A total of 57 vials of Sf9-13F12 were cryopreserved at 5×10^6 cells per mL per vial.

RNA extraction, RT-PCR, and Sanger sequencing. Total cell RNAs were prepared from a frozen cell pellet using RNeasy Plus Mini kit (Qiagen, catalogue number 74,134). Supernatant RNAs were prepared using QIAamp viral RNA mini kit (Qiagen, Germantown, MD) from 1.5 mL filtered supernatant after ultracentrifugation at 45,000 rpm (Beckman OPTIMA, TLA 45 rotor, Brea, CA) for 16 h at 4 °C and DNase I digestion (Promega, Madison, WI) for 1 h at 37 °C.

cDNAs were synthesized from cell or supernatant RNAs using iScript cDNA Synthesis Kit (Bio-rad, Hercules, CA; catalogue number 170–8890). PCR amplifications were done using a TaKaRa Ex Taq™ kit (catalogue umber RR001A, TaKaRa, Japan) and Sf-rhabdovirus specific primers (Table 1) at 94 °C for 3 min, and 35 cycles of 94 °C for 30 s, 55 °C–60 °C for 1 min, and 72 °C for 1.5 min, followed by 72 °C for 10 min.

PCR-amplified DNA fragments were isolated from agarose gels by using Zymoclean™ Gel DNA Recovery kit (Zymo Research Corp, Orange, CA; catalogue number D4001). Nucleotide sequences were determined of PCR-amplified DNA or cloned PCR-amplified DNA in the pGEM-T Easy vector (Promega; catalogue number A1360). Sequence analysis and alignment of nucleotides were done using BLAST (Altschul et al., 1990) (http://blast.ncbi.nlm.nih.gov/, National Center for Biotechnology Information, National Library of Medicine, NIH, Bethesda, MD).

Infectivity studies of Sf-rhabdovirus X^+ and X^- variants. Sf9-13F12 cells (1.6×10^6) were planted in 25-cm^2 flasks and incubated for 48 h at 28 °C. Medium was removed and 2 mL fresh medium added, into which 0.5 mL filtered supernatant (0.45 µm pore size filter) obtained from Sf9-2-20 cells or Sf9-1A3 cells at p10 (95% confluence) was inoculated. Cells were incubated for 2 h at 28 °C after which 2.5 mL complete medium was added for overnight incubation. Sf9-13F12 cells with complete medium were included as negative control. The next day, medium was removed, cell washed 3 times, and incubated with new medium added for 3–4 days at 28 °C. Cells were passaged upon reaching 95% confluence.

The cultures were regularly monitored for cytopathic effect (CPE). Filtered supernatants and washed cell pellets were collected and stored at −80 °C for RNA extraction and RT-PCR analysis.

High-throughput sequencing and bioinformatics analysis. Total cell RNA was extracted from Sf9-13F12 cell pellet at p9 using RNeasy Plus Mini kit and sent to the CBER core facility for sample processing and sequencing. RNA quality was assessed by the Agilent 2100 Bioanalyzer using the RNA 6000 Nano Kit (Agilent). The sample was processed to generate library for mRNA sequencing following the Illumina® TruSeq Stranded mRNA Sample Preparation Guide. In this method, polyA-containing mRNA was purified from 1 µg total RNA using poly-T oligo attached magnetic beads, fragmented, and reverse-transcribed into cDNAs. Double-strand cDNA was adenylated at the 3' ends and ligated to indexed sequencing adaptors, followed with a brief amplification for 15 cycles. The quality of the cDNA library was assessed by the Agilent 2100 Bioanalyzer using the DNA 1000 Kit (Agilent). One femtomole of the sequencing libraries (median size ~260 nt) was denatured and loaded onto a flow cell for cluster generation using the Illumina cBot. The sample was loaded onto one lane of a HiSeq Rapid Run flow cell. Paired-end sequencing was carried out on HiSeq 2500 sequencer (Illumina, San Diego, CA, USA) for 100 × 2 cycles. The fastq files were generated from bcl files, primary output of Illumina HiSeq using bcl2fastq module on Biowulf of NIH High Performing Computation (HPC).

The total number of paired-end reads obtained were 336,447,030, with an average length of 100-bp. The number of reads after trimming in the CLC Genomics Workbench using a Phred quality score of 20 were 330,304,690. The number of transcriptomic reads after subtracting from the Sf9 genome (Nandakumar et al., 2017) was 8,445,628. A blastn search was done (March 2018) against U-RVDB (Goodacre et al., 2018), version 12.2 (Khan and Goodacre, 2018) and sequences were selected with E-value < 1e-5. Any viral hits were followed-up to identify if the signal was a true virus hit, a cellular hit, or non-specific by mapping reads against the target virus genome as reference, with subsequent blastn analysis of the consensus sequence of the mapped reads against NCBI nr/nt and RVDB v12.2. Additionally, the presence of rhabdovirus-related sequences was specifically investigated by using exogenous Sf-rhabdovirus genes and endogenous rhabdovirus genes as reference for mapping the transcriptomic reads in the CLC genomics workbench (version 11.0; mapping parameters were: length fraction = 0.5 and similarity fraction = 0.8). The HTS reads were re-analyzed in May 2019 using the updated RVDB v15.1 (Khan and Chin, 2019). Paired HiSeq raw fastq files were processed by BBTools v38.42 (Bushnell et al., 2017) to remove the adapter sequences and low quality reads (at default settings: less than Phred quality score of 10 and length less than 40 base pairs). The processed reads were filtered by Bowtie 2 v2.3.5 (Langmead and Salzberg, 2012) using Sf9 version 2.0 draft genome (Xin et al., 2019) to remove the host cellular repetitive sequences. The host-free reads (30.44% of total reads) were analyzed using tblastx to search the clustered RVDB (C-RVDB) version 15.1 (E-value ≤1e-10).

ACCESSION NUMBER. The whole transcriptome HTS raw read data of the Sf9-13F12 cell clone has been deposited at NCBI SRA under the accession number SRP126104.

Conflicts of interest

All authors have no financial conflict of interest.

Author contributions

A.S.K. conceived and designed the study. H.M. designed and performed the laboratory experiments. E.H.B. assisted with the cell cloning. S.N. and P-J.C. performed the bioinformatics analysis. All authors were involved in various aspects of the analysis, interpretation of the results, and writing the paper. All authors had full access to the data and approved the manuscript before it was submitted by the corresponding author.

Disclaimer

The content and views expressed in this article are those of the individual authors and should not be construed to represent the views or policy of the organization, regulatory authority, or governmental agency they represent. The mention of trade names, commercial products, or organizations does not imply endorsement by the U.S. government.

Acknowledgements

We thank Norman Goodacre for help with bioinformatics analysis.

References

Altschul, S.F., Gish, W., Miller, W., Myers, E.W., Lipman, D.J., 1990. Basic local alignment search tool. J. Mol. Biol. 215, 403–410.
Bushnell, B., Rood, J., Singer, E., 2017. BBMerge - accurate paired shotgun read merging via overlap. PLoS One 12 e0185056.
Geisler, C., Jarvis, D.L., 2016. Rhabdovirus-like endogenous viral elements in the genome of Spodoptera frugiperda insect cells are actively transcribed: implications for adventitious virus detection. Biologicals 44, 219–225.
Goodacre, N., Aljanahi, A., Nandakumar, S., Mikailov, M., Khan, A.S., 2018. A Reference Viral Database (RVDB) to enhance bioinformatics analysis of high-throughput sequencing for novel virus detection. mSphere 3.
Hashimoto, Y., Macri, D., Srivastava, I., McPherson, C., Felberbaum, R., Post, P., Cox, M., 2017. Complete study demonstrating the absence of rhabdovirus in a distinct Sf9 cell line. PLoS One 12 e0175633.
Haynes, J., 2015. Methods of Detection and Removal of Rhabdovirus from Cell Lines. World Intellectual Property Organization. Takeda Vaccines, Inc.
Hink, W.F., 1970. Established insect cell line from the cabbage looper, Trichoplusia ni. Nature 226, 466–467.
Khan, A.S., Chin, P.-J., 2019. RVDB: reference virus DataBase. https://hive.biochemistry.gwu.edu/rvdb.
Khan, A.S., Goodacre, N., 2018. RVDB: reference viral DataBase. https://hive.biochemistry.gwu.edu/rvdb.
Kotin, R.M., 2011. Large-scale recombinant adeno-associated virus production. Hum. Mol. Genet. 20, R2–R6.
Langmead, B., Salzberg, S.L., 2012. Fast gapped-read alignment with Bowtie 2. Nat. Methods 9, 357–359.
Ma, H., Galvin, T.A., Glasner, D.R., Shaheduzzaman, S., Khan, A.S., 2014. Identification of a novel rhabdovirus in Spodoptera frugiperda cell lines. J. Virol. 88, 6576–6585.
Maghodia, A., Geisler, C., Jarvis, D., 2017. Virus-free Cell Lines and Methods for Obtaining Same. World Intellectual Property Organization.
Maghodia, A.B., Geisler, C., Jarvis, D.L., 2016. Characterization of an Sf-rhabdovirus-negative Spodoptera frugiperda cell line as an alternative host for recombinant protein production in the baculovirus-insect cell system. Protein Expr. Purif. 122, 45–55.
Maghodia, A.B., Jarvis, D.L., 2017. Infectivity of Sf-rhabdovirus variants in insect and mammalian cell lines. Virology 512, 234–245.
Nandakumar, S., Ma, H., Khan, A.S., 2017. Whole-genome sequence of the Spodoptera frugiperda Sf9 insect cell line. Genome Announc. 5.
Schroeder, L., Mar, T.B., Haynes, J.R., Wang, R., Wempe, L., Goodin, M.M., 2019. Host range and population survey of Spodoptera frugiperda rhabdovirus. J. Virol. 93.
Smith, G.E., Foellmer, H.G., Knell, J., DeBartolomeis, J., Voznesensky, A.I., Aug 15, 2000. Spodoptera Frugiperda Single Cell Suspension Cell Line in Serum-free Media, Methods of Producing and Using. Protein Sciences Corporation.
Summers, M.D., Smith, G.E., 1987. A Manual of Methods for Baculovirus Vectors and Insect Cell Culture Procedures. Texas Agricultural Experiment Station, College Station, TX.
US Food and Drug Adminstration, 2010. Guidance for Industry: characterizatoin and qualification of cell substrates and other biological materials used in the production of viral vaccines for infectious disease indications. http://www.fda.gov/downloads/biologicsbloodvaccines/guidancecomplianceregulatoryinformation/guidances/vaccines/ucm202439.pdf.
van Oers, M.M., Pijlman, G.P., Vlak, J.M., 2015. Thirty years of baculovirus-insect cell protein expression: from dark horse to mainstream technology. J. Gen. Virol. 96, 6–23.
Vaughn, J.L., Goodwin, R.H., Tompkins, G.J., McCawley, P., 1977. The Establishment of Two Cell Lines from the Insect Spodoptera Frugiperda (Lepidoptera; Noctuidae), vol. 13. pp. 213–217 In Vitro.
Vlak, J.M., Keus, R.J., 1990. Baculovirus expression vector system for production of viral vaccines. Adv. Biotechnol. Process. 14, 91–128.
Walker, P.J., Blasdell, K.R., Calisher, C.H., Dietzgen, R.G., Kondo, H., Kurath, G., Longdon, B., Stone, D.M., Tesh, R.B., Tordo, N., Vasilakis, N., Whitfield, A.E., Nbsp Ictv Report, C., 2018. ICTV virus taxonomy profile: rhabdoviridae. J. Gen. Virol. 99, 447–448.
Walker, P.J., Firth, C., Widen, S.G., Blasdell, K.R., Guzman, H., Wood, T.G., Paradkar, P.N., Holmes, E.C., Tesh, R.B., Vasilakis, N., 2015. Evolution of genome size and complexity in the Rhabdoviridae. PLoS Pathog. 11 e1004664.
Wickham, T.J., Davis, T., Granados, R.R., Shuler, M.L., Wood, H.A., 1992. Screening of insect cell lines for the production of recombinant proteins and infectious virus in the baculovirus expression system. Biotechnol. Prog. 8, 391–396.
Xin, G., Chin, P.-J., Khan, A.S., 2019. Spodoptera Frugiperda Sf9 Draft Genome. version 2.0. in preparation.